Structural Engineering and Mechanics, Vol. 42, No. 3 (2012) 313-334 313
DOI: http://dx.doi.org/10.12989/sem.2012.42.3.313

Exact and complete fundamental solutions for penny-shaped crack in an infinite transversely isotropic thermoporoelastic medium: mode I problem

Xiang-Yu LI*[1,2], J. Wu[3], W.Q. Chen[4], Hui-Ying Wang[5] and Z.Q. Zhou[6]

[1]*School of Mechanics and Engineering, Southwest Jiaotong University, Chengdu, 610031, P.R. China*
[2]*UPMC Sisyphe, Boîte 105, 4 Place Jussieu, 75252 Paris, Cedex 05, France*
[3]*Laboratoire d'Etudes Aérodynamiques, Université de Poitiers, Bd Marie et Pierre Curie, BP 30179, Téléport 2, Chasseneuil, Cedex, France*
[4]*Department of Engineering Mechanics, Zhejiang University, Yuquan Campus, Hangzhou 310027, P.R. China*
[5]*E.N.S.M.A., University of Poitiers, B.P., B.P. 109-Chasseneuil du Poitou 86960 Futuroscope, Cedex, France*
[6]*Department of Mechanical and Aerospace Engineering, University of Miami, Coral Gables, FL 33124, USA*

(Received January 5, 2011, Revised March 9, 2012, Accepted March 24, 2012)

Abstract. This paper examines the problem of a penny-shaped crack in a thermoporoelastic body. On the basis of the recently developed general solutions for thermoporoelasticity, appropriate potentials are suggested and the governing equations are solved in view of the similarity to those for pure elasticity. Exact and closed form fundamental solutions are expressed in terms of elementary functions. The singularity behavior is then discussed. The present solutions are compared with those in literature and an excellent agreement is achieved. Numerical calculations are performed to show the influence of the material parameters upon the distribution of the thermoporoelastic field. Due to its ideal property, the present solution is a natural benchmark to various numerical codes and simplified analyses.

Keywords: thermoporoelasticity; transversely isotropic; fundamental solution; potential theory method; penny-shaped crack

1. Introduction

Biot (1941) proposed the theory of poroelasticity to study the coupling behavior of two-phase media. This triggered tremendous academic interests in the following 70 years. On the basis of the generalized Hooke's law, Biot (1955) developed the theory of anisotropic poroelasticity. To account for the thermal effect, arising in deep drilling and nuclear storage facilities, thermoporoelasticity model was founded (Coussy 1995, Abousleiman and Ekbote 2000).

Fundamental solutions in poroelasticity, due to its practical significance, have been a hot point in the last decades. Following the work of Nowacki (1966), Cleary (1977) derived the fundamental

*Corresponding author, Ph.D., E-mail: zjuparis6@hotmail.com

solutions for quasi-static problem. Then, Cheng and Liggett (1984a, b) employed Laplace transform to derive a quasi-static poroelastic fundamental solution. Later, time harmonic Green's functions were given by Norris (1985). Chen (1994a, b) derived the time domain Green's functions for two- and three-dimensional dynamic poroelastic problems. More recently, Gatmiri and Nguyen (2005) presented closed-form fundamental solutions for two-dimensional saturated soil with incompressible fluid. The state-of-the-art in fundamental solutions in poroelasticity was comprehensively reviewed by Gatmiri and Jabari (2005a, b), who also pointed out the merits and drawbacks of the previous works.

The crack problems enjoy a high level of popularity in both thermoelasticity and poroelasticity. Boone and Detournay (1990) investigated the response of a vertical crack contained in a semi-infinite impermeable elastic layer. The plain strain fracture problems of poroelasticity were studied by Atkinson and Craster (1991). Gordeyev (1995) examined a disk-shaped crack in a transversely isotropic poroelastic material saturated with fluid. Adélaïde *et al.* (2003) presented an analytic solution of hydrostatic-elastic problem considering the interaction of wetting fluid with a penny-shaped circular crack. For an axisymetrically loaded external circular crack located in a transversely isotropic medium, Singh *et al.* (1987) examined the thermoelastic behavior via Hankel transform. Recently, Liu and Kardomateas (2005) utilized two-dimensional theory of anisotropic thermoelasticity and conducted a solution for the thermal stress intensity factors due to the obstruction of a uniform heat flux by an insulated line crack. It is seen that most of the previous works was limited to two-dimensional analyses (Gordeyev 1995, Liu and Kardomateas 2005, to name a few) or to isotropic cases (Boone and Detournay 1990, Atkinson and Craster 1991, etc.). Combining the general thermoelastic solutions with the potential theory method initiated by Fabrikant (1989), Chen *et al.* (2004) derived fundamental solutions of a penny-shaped crack problem subject to a point temperature load, which made a breakthrough in crack analyses in thermoelasticity. For advances before 2004 in potential theory analyses of multi-field coupled problems, the reader is referred to the review article by Chen and Ding (2004).

Exact analyses play an important role in digging out the physical essence of the problem, hence benchmarks to numerical codes and simplified models. There are some analytical solutions, such as Gibson's footing (Gibson 1967, Gibson and McNamme 1968) and Mandel problems (Cheng and Detournay 1988, Abousleiman *et al.* 1996), which can be relied on for validating finite element implementations for modeling poroelasticity. More recently, Li *et al.* (2010) provided another one for a uniformly loaded penny-shaped crack contained in a thermoporoelastic medium. Li *et al.* (2010) considered that axisymmetric problem to discuss the validity of the general solutions and pointed out that the nonaxisymmetric problem can be also treated by the method present therein. In this sense, the present paper is a continuation yet a promotion of the previous work. Moreover, to the authors' best knowledge, no three-dimensional fundamental solutions for a thermoporoelastic medium containing a penny-shaped crack were reported in literature.

This paper aims to develop an exact 3D analysis for a penny-shaped crack under the action of point mechanical, thermal and pressure loads applied symmetrically on the crack surfaces. Due to the symmetry characteristic, the original problem is transformed into a mixed boundary-value problem of a half space. Then appropriate potential functions are given and the governing integral and integro-differential equations are presented. In view of the mathematical similarity of the governing equations to those available in literature, the equations are successfully solved. The exact and closed-form fundamental solutions in terms of elementary functions are derived via the superposition principle. The behavior of the crack tip is analyzed and the stress intensity factor is given explicitly. The validity of the present solutions is studied both analytically and numerically. An excellent agreement has been observed. Numerical calculation is performed to investigate the effect of material properties on the thermoporoelastic field. In view of the rareness of the exact solutions in thermoporoelasticity, the present results can serve as a benchmark to various numerical codes and approximate analyses.

2. Governing equations

The constitutive equations of transversely isotropic thermoporoelastic media are given by Coussy (1995) and are listed in Appendix A. The equations governing the displacement field can be easily derived by inserting Eq. (A1) into the equilibrium equations in terms of stress components. Introducing a complex displacement $U = u+iv(i=\sqrt{-1})$, these governing equations can be put in a compact form as

$$\left(\frac{c_{11}+c_{66}}{2}\Delta+c_{44}\frac{\partial^2}{\partial z^2}\right)U+\frac{c_{11}-c_{66}}{2}\Lambda^2\overline{U}+(c_{13}+c_{44})\Lambda\frac{\partial w}{\partial z}-\Lambda(\alpha_1 P+\beta_1 T) = 0$$

$$\left(c_{44}\Delta+c_{33}\frac{\partial^2}{\partial z^2}\right)w+\frac{1}{2}(c_{13}+c_{44})\frac{\partial}{\partial z}(\overline{\Lambda}U+\Lambda\overline{U})-\frac{\partial}{\partial z}(\alpha_3 P+\beta_3 T) = 0 \tag{1}$$

where $\Delta = \partial^2/\partial x^2+\partial^2/\partial y^2$, $\Lambda = \partial/\partial x+i\partial/\partial y$ and the overbar denotes the complex conjugate value. The physical meanings of all the quantities involved in Eq. (1) are given in Appendix A.

Assuming that the rate of both fluid mass content and entropy vanishes and that the loading involved varies slowly with time, we employ an uncoupled thermoporoelastic theory. Hence, if the medium is in a steady-state, the equations governing the pressure and temperature fields are the following two quasi-Laplace equations

$$\left(\kappa_{11}\Delta+\kappa_{33}\frac{\partial^2}{\partial z^2}\right)P = 0 \tag{2}$$

$$\left(\lambda_{11}\Delta+\lambda_{33}\frac{\partial^2}{\partial z^2}\right)T = 0 \tag{3}$$

where $\kappa_{11}(\kappa_{33})$ and $\lambda_{11}(\lambda_{33})$ are coefficients of permeability and thermal conductivity.

3. General solution

The general solution to Eqs. (1)-(3), recently developed by Li *et al.* (2010), can be recast into the following form

$$U = -\Lambda\left(\Phi_0+\sum_{j=1}^{4}\Phi_j\right),\quad w = \sum_{j=1}^{4}\mu_{j1}\frac{\partial\Phi_j}{\partial z_j},\quad P=\sum_{j=1}^{4}\mu_{j2}\frac{\partial^2\Phi_j}{\partial z_j^2},\quad T=\sum_{j=1}^{4}\mu_{j3}\frac{\partial^2\Phi_j}{\partial z_j^2} \tag{4}$$

where $z_j = s_j z$ $(j = 1-4)$, $s_3 = \sqrt{\kappa_{11}/\kappa_{33}}$, $s_4 = \sqrt{\lambda_{11}/\lambda_{33}}$ and $s_j(j=1,2)$ are the roots with a positive real part of the following algebraic equation (Ding *et al.* 2006)

$$a_0 s^4 - b_0 s^2 + c_0 = 0 \tag{5}$$

The constants contained in Eqs. (4) and (5) are listed in Appendix B. The potential functions $\Phi_j (j = 0-4)$ in Eq. (4) are quasi harmonic functions, i.e.

$$\left(\Delta + \frac{\partial^2}{\partial z_i^2}\right)\Phi_i = 0, \quad (i = 0, 1, \ldots, 4) \tag{6}$$

with $z_0 = s_0 z$ and $s_0 = \sqrt{c_{66}/c_{44}}$.

It should be pointed out that the general solution presented in Eq. (4) is valid only for the case of distinct $s_j (j = 1-4)$. Different forms should be utilized for other cases. A detailed discussion can be found in Li *et al.* (2010).

From Eqs. (A1) and (4), we can derive the expressions of the stress field

$$\sigma_z = \sum_{j=1}^{4} \gamma_{j1} \frac{\partial^2 \Phi_0}{\partial z_j^2}, \quad \sigma_1 = \sum_{j=1}^{4} \gamma_{j2} \frac{\partial^2 \Phi_j}{\partial z_j^2}$$

$$\sigma_2 = -2c_{66}\Lambda^2\left(\sum_{j=1}^{4} \Phi_j + i\Phi_0\right), \quad \tau_z = \Lambda\left(\sum_{j=1}^{4} \gamma_{j3} \frac{\partial \Phi_j}{\partial z_j} - ic_{44}s_0 \frac{\partial \Phi_0}{\partial z_0}\right) \tag{7}$$

where $\sigma_1 = \sigma_x + \sigma_y$, $\sigma_2 = \sigma_x - \sigma_y + 2i\sigma_{xy}$, $\tau_z = \sigma_{zx} + i\sigma_{yz}$ and the constants γ_{ji} are given in Appendix B.

As pointed out by Li *et al.* (2010), three-dimensional analyses of the mixed boundary-value problems associated with cracks and punches by virtue of the potential theory method proposed by Fabrikant (1989) can be conveniently conducted on the basis of the general solution. To show the practical significance of the potential theory method conjugated with the general solution in Li *et al.* (2010), we consider in the following section a penny-shaped crack which is embedded in an infinite thermoporoelastic medium

4. Generalized potential theory method for penny-shaped crack problem

We now consider a penny-shaped crack with its surface parallel to the plane of isotropy contained in an infinite thermoporoelastic medium (see Fig. 1). We also assume that the characteristic length a_0 of the borehole is far less than the crack radius a, hence neglect the borehole effect. A cylindrical coordinate system (ρ, ϕ, z) is so constructed that the plane $z = 0$ (denoted by I hereafter) coincides with the crack surface and the origin is located at the center of the crack. In the following analyses, the symbols S and $\bar{S}$ denote the crack and its exterior regions. Furthermore, the identities $S \cup \bar{S} = I$ and $S \cap \bar{S} = \varnothing$ hold, implying neither separation nor overlap between S and $\bar{S}$. It is assumed that a concentrated force $2\pi\Theta_1^0$, a point pressure load Θ_2^0 and a point thermal load Θ_3^0 are symmetrically applied at the points $(\rho_0, \phi_0, 0^{\pm})$ on the crack surfaces. Here, the factor 2π is introduced for the algebraic convenience and the superscript 0 indicates prescribed values. Taking advantage of the symmetrical conditions, we can formulate the original problem as a mixed boundary-value problem of the upper half space $z \geq 0$, subject to the following boundary conditions at $z = 0$

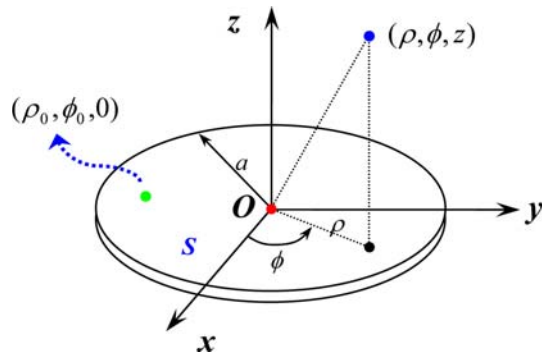

Fig. 1 A schematic diagram for a penny-shaped crack and the coordinate systems. S represents the subsection occupied by the penny shaped crack

$$(\rho,\phi)\in S{:}[\sigma_z\ \ P\ \ T] = [2\pi\Theta_1^0\ \ \Theta_2^0\ \ \Theta_3^0]\delta(\rho-\rho_0,\phi-\phi_0)/\rho$$
$$(\rho,\phi)\in \bar{S}{:}w = 0,\ \frac{\partial P}{\partial z} = 0,\ \frac{\partial T}{\partial z} = 0$$
$$(\rho,\phi)\in I{:}\ \tau_z = 0 \tag{8}$$

where δ is the well known Dirac Delta function.

The problem can be solved if appropriate potential functions are found. To this end, we assume that

$$\Phi_0 = 0,\quad \Phi_i = \sum_{j=1}^{3} e_{ij}\Omega_j(\rho,\phi,z_i)\ ,\quad (i=1-4) \tag{9}$$

where e_{ij} are constants to be determined, and

$$\Omega_1(M) = \iint_S \frac{\omega_1(N)}{R(M,N)}dS_N$$
$$\Omega_j(M) = \iint_S \omega_j(N)\{z\ln[R(M,N)+z]-R(M,N)\}dS_N,\quad (j=2,3) \tag{10}$$

where ω_1, ω_2 and ω_3 are the crack opening displacement $w(\rho,\phi,0)$, pressure gradient $\partial P(\rho,\phi,z)/\partial z|_{z=0}$ and temperature gradient $\partial T(\rho,\phi,z)/\partial z|_{z=0}$, respectively; $R(M,N_0)$ is the distance between the points $M(\rho,\phi,z)$ and $N(r,\theta,0)$. Hereafter $R(\text{o},\text{o})$ represents the distance between the corresponding points.

All the zero boundary conditions in Eq. (8) can be met by setting

$$\begin{Bmatrix} e_{1j} \\ e_{2j} \\ e_{3j} \\ e_{4j} \end{Bmatrix} = -\frac{1}{2\pi}\begin{bmatrix} \gamma_{13} & \gamma_{23} & \gamma_{33} & \gamma_{43} \\ \mu_{11} & \mu_{21} & \mu_{31} & \mu_{41} \\ \mu_{12}s_1 & \mu_{22}s_2 & \mu_{32}s_3 & \mu_{42}s_4 \\ \mu_{13}s_1 & \mu_{23}s_2 & \mu_{33}s_3 & \mu_{43}s_4 \end{bmatrix}^{-1}\begin{Bmatrix} 0 \\ \delta_{1j} \\ \delta_{2j} \\ \delta_{3j} \end{Bmatrix},\quad (j=1,2,3) \tag{11}$$

where δ_{ij} is the Kronecker delta. The satisfaction of the non-zero boundary conditions leads to

$$m_{11}\Delta\iint_S \frac{\omega_1(N)}{R(N,N_0)}dS_N - \sum_{j=2}^{3} m_{1j}\iint_S \frac{\omega_j(N)}{R(N,N_0)}dS_N = -2\pi\Theta_1^0\delta(\rho-\rho_0,\phi-\phi_0)/\rho \quad (12)$$

$$\iint_S \frac{\omega_j(N)}{R(N,N_0)}dS_N = -2\pi s_{j+1}\Theta_j^0\delta(\rho-\rho_0,\phi-\phi_0)/\rho, \quad (j=2,3) \quad (13)$$

where $m_{1j} = \sum_{i=1}^{4}\gamma_{i1}e_{ij}$, $(j=1,2,3)$ and $N_0(\rho_0,\phi_0,0)\in S$. Making use of Eq. (13), we arrive at

$$\Delta\iint_S \frac{\omega_1(N)}{R(N,N_0)}dS_N = -2\pi\overline{\Theta}_1^0\delta(\rho-\rho_0,\phi-\phi_0)/\rho \quad (14)$$

where

$$\overline{\Theta}_1^0 = [\Theta_1^0 + m_{12}s_3\Theta_2^0 + m_{13}s_4\Theta_3^0]/m_{11} \quad (15)$$

which can be viewed as the generalized mechanical load. Here, we just list the main results and a detailed derivation has been given by Li *et al.* (2010).

Because of the uncoupled theory adopted in the present study, the presence of pressure and thermal loadings will result in a variation of the elastic field (see Eqs. (14) and (15)), while the mechanical loading contributes nothing to the thermal and pressure fields (see Eq. (13)). Moreover, no mutual effects can be observed between the thermal and pressure fields. As a result, the uncoupled character provides us a way to discuss the validity of the solutions in this paper by comparing with those in literature. This purpose can be easily fulfilled by setting $\Theta_2^0 = 0$ ($\Theta_3^0 = 0$). Under that condition, the present solutions readily degenerate to those to the crack problems in thermoelasticity (poroelasticity).

It has been pointed out by Li *et al.* (2010) that the integral Eq. (13) and integro-differential Eq. (14) have the same mathematical structures as those for contact and crack problems in pure elasticity, respectively. Due to this similarity, the delicate results given by Fabrikant (1989, 1991) can be used directly to solve the governing Eqs. (13) and (14). This is the topic of the next section.

5. Potential functions

Through a comparison with the results in Fabrikant (1989), the solutions to Eqs. (13) and (14) can be obtained

$$\omega_1(\rho,\phi) = \frac{\overline{\Theta}_1^0}{\pi^2}\int_\rho^a \frac{dx}{\sqrt{x^2-\rho^2}}\int_0^x \frac{dy}{\sqrt{x^2-y^2}}L\left(\frac{\rho y}{x^2}\right)\delta(y-\rho_0,\phi-\phi_0) \quad (16)$$

$$\omega_j(\rho,\phi) = \frac{2\Theta_j^0 s_{j+1}}{\pi\rho}L(\rho)\frac{d}{d\rho}\int_\rho^a \frac{x\,dx}{\sqrt{x^2-\rho^2}}L\left(\frac{1}{x^2}\right)\frac{d}{dx}\int_0^x \frac{dy}{\sqrt{x^2-y^2}}L(y)\delta(y-\rho_0,\phi-\phi_0) \quad (17)$$

where $j = 2,3$ and $L(\bullet)$ is an operator with the following definition

$$L(k)f(\phi) = \frac{1}{2\pi}\int_0^{2\pi}\frac{(1-k^2)f(\phi_0)}{1-2k\cos(\phi-\phi_0)+k^2}d\phi_0, \quad (0\le k<1) \tag{18}$$

The integrals in Eqs. (16) and (17) are deliberately put in identical forms to those in elasticity without any simplification by virtue of the property of Dirac Delta function. This is just because of the purpose of using Fabrikant's results by an analog.

Inserting Eq. (16) into Eq. $(10)_1$ gives arise to

$$\Phi_1(\rho,\phi,z) = \frac{\overline{\Theta}_1^0}{\pi^2}\int_0^{2\pi}\int_0^a \Pi_1(\rho,\phi,z;\rho_0,\phi_0)\delta(\rho-\rho_0,\phi-\phi_0)d\rho_0 d\phi_0 \tag{19}$$

It is evident that $\Pi_1(\rho,\phi,z;\rho_0,\phi_0)$ is a Green's function, whose expression has been shown in Fabrikant (1989) as

$$\Pi_1(M;N_0) = \Pi_1(\rho,\phi,z;\rho_0,\phi_0) = \int_0^{2\pi}\int_0^a \frac{1}{R(N,N_0)}\tan^{-1}\left[\frac{\sqrt{a^2-\rho^2}\sqrt{a^2-\rho_0^2}}{aR(N,N_0)}\right]\frac{rdrd\theta}{R(M,N)} \tag{20}$$

Although unable to compute $\Pi_1(M;N_0)$ in terms of elementary functions, the derivatives of various orders necessary for evaluating the thermoporoelastic field are listed in Appendix C, for the sake of the completeness of the present paper.

Substitution of Eq. (17) into Eq. $(10)_2$ results in

$$\Phi_j = -\frac{2s_{j+1}}{\pi}\int_0^{2\pi}\int_0^a \Pi_2(\rho,\phi,z;\rho_0,\phi_0)\delta(\rho-\rho_0,\phi-\phi_0)d\rho_0 d\phi_0, \quad (j=2,3) \tag{21}$$

As pointed out by Chen *et al.* (2004), the explicit form of Π_2 is very difficult to obtain. However, we can express Π_2 by an integral whose integrand can be given in terms of elementary functions, i.e.

$$\Pi_2(M;N_0) = \Pi_2(\rho,\phi,z;\rho_0,\phi_0) = \int \Xi(M;N_0)dz \tag{23}$$

where

$$\Xi(M;N_0) = -\frac{1}{R(M,N_0)}\tan^{-1}\left[\frac{\sqrt{a^2-\rho^2}\sqrt{a^2-\rho_0^2}}{aR(M,N_0)}\right] + \frac{1}{\sqrt{a^2-\rho_0^2}}\left[\ln\left(\frac{a+\sqrt{a^2-l_1^2}}{l_1}\right)\right.$$
$$\left. + \frac{1}{\sqrt{\varsigma-1}}\tan^{-1}\left(\frac{\sqrt{a^2-l_1^2}}{a\sqrt{\varsigma-1}}\right) + \frac{1}{\sqrt{\bar{\varsigma}-1}}\tan^{-1}\left(\frac{\sqrt{a^2-l_1^2}}{a\sqrt{\bar{\varsigma}-1}}\right)\right] \tag{23}$$

with $\varsigma = \rho e^{i(\phi-\phi_0)}/\rho_0$ and l_1 is defined in Appendix C.

At this stage, the partial derivatives with respect to the spatial coordinates of the Green's functions Π_j, $(j=1,2)$ are available (Chen *et al.* 2004), so we can conduct the exact and complete fundamental thermoporoelastic solutions in the following section.

6. Exact fundamental thermoporoelastic solution

In view of the structure of Eq. (9), we separate the thermoporoelastic field into two parts. The first part corresponds to the potential function Ω_1 and the second part to Ω_j $(j = 2, 3)$. We can combine Ω_2 and Ω_3 together, because of the similarity between the temperature and pressure fields. For the problem concerned in the present study, we can derive the thermoporoelastic field **X** (say) by employing directly the results shown in Fabrikant (1989) and Chen *et al.* (2004). **X** can be expressed as the sum of two terms

$$\mathbf{X} = \mathbf{X}^{(1)} + \mathbf{X}^{(2)} \tag{24}$$

where $\mathbf{X} = [U \;\; w \;\; \sigma_z \;\; \sigma_1 \;\; \sigma_2 \;\; P \;\; T]^t$ and

$$\begin{aligned}
U^{(1)} &= \frac{2\overline{\Theta}_1^0}{\pi}\sum_{i=1}^{4} e_{i1} f_1(z_i), & w^{(1)} &= -\frac{2\overline{\Theta}_1^0}{\pi}\sum_{i=1}^{4} \mu_{i1} e_{i1} f_2(z_i) \\
\sigma_z^{(1)} &= -\frac{2\overline{\Theta}_1^0}{\pi}\sum_{i=1}^{4} \gamma_{i1} e_{i1} f_3(z_i), & \sigma_1^{(1)} &= -\frac{2\overline{\Theta}_1^0}{\pi}\sum_{i=1}^{4} \gamma_{i3} e_{i1} f_3(z_i) \\
\sigma_2^{(1)} &= \frac{4c_{66}\overline{\Theta}_1^0}{\pi}\sum_{i=1}^{4} e_{i1} f_4(z_i), & \tau_z^{(1)} &= -\frac{2\overline{\Theta}_1^0}{\pi}\sum_{i=1}^{4} \gamma_{i3} e_{i1} f_5(z_i) \\
P^{(1)} &= -\frac{2\overline{\Theta}_1^0}{\pi}\sum_{i=1}^{4} \mu_{i2} e_{i1} f_3(z_i), & T^{(1)} &= -\frac{2\overline{\Theta}_1^0}{\pi}\sum_{i=1}^{4} \mu_{i3} e_{i1} f_3(z_i)
\end{aligned} \tag{25}$$

$$\begin{aligned}
U^{(2)} &= \frac{2}{\pi}\sum_{k=2}^{3} s_{k+1}\Theta_k^0 \sum_{i=1}^{4} e_{ik} g_1(z_i), & w^{(2)} &= -\frac{2}{\pi}\sum_{k=2}^{3} s_{k+1}\Theta_k^0 \sum_{i=1}^{4} \mu_{i1} e_{ik} g_2(z_i) \\
\sigma_z^{(2)} &= -\frac{2}{\pi}\sum_{k=2}^{3} s_{k+1}\Theta_k^0 \sum_{i=1}^{4} \gamma_{i1} e_{ik} g_3(z_i), & \sigma_1^{(2)} &= -\frac{2}{\pi}\sum_{k=2}^{3} s_{k+1}\Theta_k^0 \sum_{i=1}^{4} \gamma_{i2} e_{ik} g_3(z_i) \\
\sigma_2^{(2)} &= \frac{4c_{66}}{\pi}\sum_{k=2}^{3} s_{k+1}\Theta_k^0 \sum_{i=1}^{4} e_{ik} g_4(z_i), & \tau_z^{(2)} &= -\frac{2}{\pi}\sum_{k=2}^{3} s_{k+1}\Theta_k^0 \sum_{i=1}^{4} \gamma_{i3} e_{ik} g_5(z_i) \\
P^{(2)} &= -\frac{2}{\pi}\sum_{k=2}^{3} s_{k+1}\Theta_k^0 \sum_{i=1}^{4} \mu_{i2} e_{ik} g_3(z_i), & T^{(2)} &= -\frac{2}{\pi}\sum_{k=2}^{3} s_{k+1}\Theta_k^0 \sum_{i=1}^{4} \mu_{i3} e_{ik} g_3(z_i)
\end{aligned} \tag{26}$$

The functions $f_i(z)$ and $g_i(z)$ $(i = 1-5)$, which are closely related to the derivatives of the Green's functions, are given in Appendix C.

At the first sight, the formulae seem to contradict with the uncoupled theory employed herein in two aspects: (1) the generalized mechanical load $\overline{\Theta}_1^0$ would give rise to a variation in both temperature and pressure fields (see Eq. (25)); (2) the temperature and pressure fields would have a mutual effect (see Eq. (26)). However, this contradiction is actually not true. Using the relations in Eq. (11) and noticing $\mu_{i2} = 0$, $\mu_{j3} = 0$ $(i = 1, 2, 4; j = 1, 2, 3)$, we can immediately get

$$P^{(1)} = 0\,, \quad T^{(1)} = 0\,, \quad P^{(2)} = \frac{\Theta_2^0}{\pi^2} g_3(z_3)\,, \quad T^{(2)} = \frac{\Theta_3^0}{\pi^2} g_3(z_4) \tag{27}$$

which definitively removes the seeming contradiction.

Of course, we can obtain the fundamental pressure and temperature fields independently by using the potential theory method to solve the corresponding mixed boundary-value problem. For an arbitrarily distributed pressure load $\Theta_2(\rho_0, \phi_0)$ acting on the crack surface, Li *et al.* (2010) showed that

$$P(\rho, \phi, z) = \frac{1}{\pi^2}\int_0^{2\pi}\int_0^a \left[\frac{R'}{h} + \tan^{-1}\left(\frac{h}{R'}\right)\right]\frac{z_3}{(R')^3}\Theta_2(r, \theta) r\,dr\,d\theta \tag{28}$$

with $R' = \sqrt{\rho^2 + r^2 - 2\rho r\cos(\phi - \theta) + z_3^2}$. On letting $\Theta_2(r, \theta) = \Theta_2^0\delta(r - \rho_0, \theta - \phi_0)/r$, we immediately arrive at the expression of $P(\rho, \phi, z)$ in Eq. (27), hence validating the present pressure field. The temperature can be verified in the same manner.

Once the complete thermoporoelastic field is available, we can examine the singular behavior at the tip of a penny-shaped crack under the action of point loads lactating at an arbitrary point on the crack surface. Taking advantage of the following property

$$l_1\big|_{z=0} = l_1(\rho, a, 0) = \min(a, \rho)\,, \quad l_2\big|_{z=0} = l_2(\rho, a, 0) = \max(a, \rho) \tag{29}$$

we can derive from Eqs. (25) and (26) that

$$(\rho, \phi, 0) \in \bar{S}\colon\ \sigma_z = \sigma_z^{(1)} + \sigma_z^{(2)} \tag{30}$$

where

$$\sigma_z^{(1)} = -\frac{2\bar{\Theta}_1^0}{\pi} m_{11}\sqrt{\frac{a^2 - \rho_0^2}{\rho^2 - a^2}}\frac{1}{\rho^2 + \rho_0^2 - 2\rho\rho_0\cos(\phi - \phi_0)}$$

$$\sigma_z^{(2)} = -\frac{2}{\pi}\left(\sum_{k=2}^{3} m_{1k}s_{k+1}\Theta_k^0\right)\sqrt{\frac{\rho^2 - a^2}{a^2 - \rho_0^2}}\frac{1}{\rho^2 + \rho_0^2 - 2\rho\rho_0\cos(\phi - \phi_0)} \tag{31}$$

Now it is evident that $\sigma_z^{(1)}$ and $\sigma_z^{(2)}$ respectively tend to ∞ and 0 as $\rho \to a^+$. This observation is similar to the crack problem in pure elasticity (Fabrikant 1989).

If the stress intensity factor is defined as

$$K_I = \lim_{\rho \to a^+}\sqrt{2\pi(\rho - a)}\,\sigma_z\big|_{z=0} \tag{32}$$

then we derive that

$$K_i = -\frac{2(\Theta_1^0 + s_3 m_{12}\Theta_2^0 + s_4 m_{13}\Theta_3^0)}{\sqrt{\pi a}}\frac{\sqrt{a^2 - \rho_0^2}}{a^2 + \rho_0^2 - 2a\rho_0\cos(\phi - \phi_0)} \tag{33}$$

where Eq. (15) has been used.

If the mechanical load Θ_1^0 is solely considered, Eq. (25) agrees with Fabrikant's result in elasticity. Setting $\Theta_1^0 = 0$ and $\Theta_2^0 = 0$, we get the same result as Chen *et al.* (2004) with an exception of coefficients. However, for a specific material, numerical computation reveals an excellent agreement, which will be shown later.

At the present stage, we have at least two ways to check the validity of the present solutions. The first choice is to construct the thermoporoelastic field for a uniformly loaded crack by integrating the corresponding physical quantities in Eqs. (24)-(27). The results thus obtained are then compared with those in Li *et al.* (2010), who has treated this special case. The other option is to set Θ_1^0 and Θ_2^0 to zero and compare the solutions to those given by Chen *et al.* (2004). The following sections will be devoted to the validity of the present solutions.

7. Uniformly loaded crack

Now consider a penny-shaped crack under the action of uniformly distributed mechanical, thermal and pressure loads, i.e., $\forall(\rho, \phi, 0) \in S$: $\sigma_z(\rho, \phi, 0) = Q_1^0$, $P(\rho, \phi, 0) = Q_2^0$ and $T(\rho, \phi, 0) = Q_3^0$, where $Q_j^0 (j = 1-3)$ is a prescribed constant. For convenience, the symbol $\overline{Q}_1^0$ equal to $[Q_1^0 + m_{12}s_3Q_2^0 + m_{13}s_4Q_3^0]/m_{11}$ is introduced to denote the generalized mechanical load. The thermoporoelastic field in this case can be derived through an integration of the corresponding fundamental solutions in the previous section, for example

$$U = \frac{2\overline{Q}_1^0}{\pi}\sum_{i=1}^{4} e_{i1}\iint_S f_1(z_1)dS + \frac{2}{\pi}\sum_{k=2}^{3} s_{k+1}Q_k^0\sum_{i=1}^{4} e_{ik}\iint_S g_1(z_i)dS$$

$$w = -\frac{2\overline{Q}_1^0}{\pi}\sum_{i=1}^{4} \mu_{i1}e_{i1}\iint_S f_2(z_i)dS - \frac{2}{\pi}\sum_{k=2}^{3} s_{k+1}Q_k^0\sum_{i=1}^{4} \mu_{i1}e_{ik}\iint_S g_2(z_i)dS$$

$$P = \frac{Q_2^0}{\pi^2}\iint_S g_3(z_3)dS, \quad T = \frac{Q_3^0}{\pi^2}\iint_S g_3(z_4)dS$$

$$K_I = -\frac{2\overline{Q}_1^0}{\sqrt{\pi a}}\iint_S \frac{\sqrt{a^2-\rho_0^2}}{a^2+\rho_0^2-2a\rho_0\cos(\phi-\phi_0)}dS \tag{34}$$

From Eq. (33), we obtain that

$$U = 2\overline{Q}_1^0\rho e^{i\phi}\sum_{j=1}^{4} e_{j1}\left[\sin^{-1}\left(\frac{a}{l_{2j}}\right) - \frac{a\sqrt{l_{2j}^2-a^2}}{l_{2j}^2}\right]$$

$$-4\frac{e^{i\phi}}{\rho}\sum_{k=2}^{3} s_{k+1}Q_k^0\sum_{j=1}^{4} e_{ik}\left[\sqrt{l_{2j}^2-a^2}\left(a-\frac{l_{1j}^2}{2a}\right) - az_j + \frac{\rho^2}{2}\sin^{-1}\left(\frac{a}{l_{2j}}\right)\right]$$

$$w = 4\overline{Q}_1^0\sum_{j=1}^{4} \mu_{j1}e_{j1}\left[z_j\sin^{-1}\left(\frac{a}{l_{2j}}\right) - \sqrt{a^2-l_{1j}^2}\right]$$

$$-4\sum_{k=2}^{3} s_{k+1}Q_k^0\sum_{j=1}^{4} \mu_{j1}e_{jk}\left[z_j\sin^{-1}\left(\frac{a}{l_{2j}}\right) - \sqrt{a^2-l_{1j}^2} + a\ln(l_{2j} + \sqrt{l_{2j}^2-\rho^2})\right]$$

$$P = \frac{2}{\pi}Q_2^0 \sin^{-1}\left(\frac{a}{l_{23}}\right), \quad T = \frac{2}{\pi}Q_3^0 \sin^{-1}\left(\frac{a}{l_{24}}\right)$$

$$K_I = -4m_{11}\overline{\Theta}_1^0\sqrt{\pi a} \tag{35}$$

where $l_{ij} = l_{ij}(a, \rho, z_j)$, $(i = 1, 2, j = 1-4)$ are defined in Eq. (C2). The results in Eq. (34) are identical to those presented in Li *et al.* (2010). Although the integrals involved in Eq. (34) are quite tedious, however they are basic and the handbook (Gradsbteyn and Ryzbik 2004) is very useful to work them out.

8. Numerical results and discussions

Numerical results are present in this section, which consists of two parts. The first part is devoted to the verification of the theomoporoelastic field presented in previous sections. The other part studies the influence of the anisotropy of media on the corresponding physical quantities in terms of the ratios E'/E and ν'/ν, which characterize the anisotropy of the porous media.

In the following analyses, the loads under consideration are applied at the point $(\rho_0, \phi_0) = (0.5a, 0)$. The radius of the crack a and the Young's modulus E in the isotropic plane are respectively taken to be the reference scales of the length and stress.

It is stressed that all the numerical calculations involved were performed under the condition $s_i \neq s_j$, $(i \neq j)$.

8.1 Verification of the themoporoelastic field

To show the consistency of the present solutions with Chen *et al.* (2004), we made numerical calculations for a penny-shaped crack subjected to a point thermal load $\Theta_3^0 = 1$ ºC only. Table 1 gives the material constants for a deep-water Gulf shale of Mexico (Kanj and Abousleiman 2005), whose physical meanings are given in Appendix A. In this case, the solution in the section should be identical to those given by Chen *et al.* (2004), as pointed out in section 6.

Table 1 Material parameters used in numerical analysis

Parameter	Value	Unit
E (E')	1854 (927)	[MPa]
G'	185.40	[MPa]
ν (ν')	0.22 (0.44)	-
κ_{11} (κ_{33})	0.1 (0.3)	$\left[\frac{D}{\text{Pa s}}\right]$
λ_{11} (λ_{33})	2.65 (4.00)	$\left[\frac{\text{W}}{{}^\circ\text{C m}}\right]$
$\alpha_1^s(\alpha_3^s)$	6×10^{-6} (1.2×10^{-5})	$\left[\frac{1}{{}^\circ\text{C}}\right]$

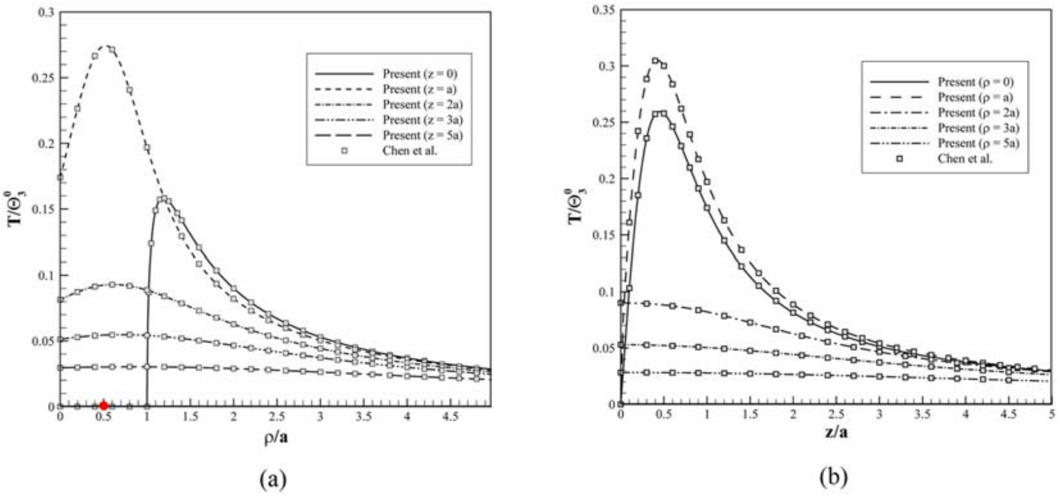

Fig. 2 The dimensionless temperature T/Θ_3^0 as a function of (a) ρ/a and of (b) z/a. In (a), the mark (•) denotes the position where the point load is applied. The corresponding T/Θ_3^0 is 1, which is not shown for simplicity

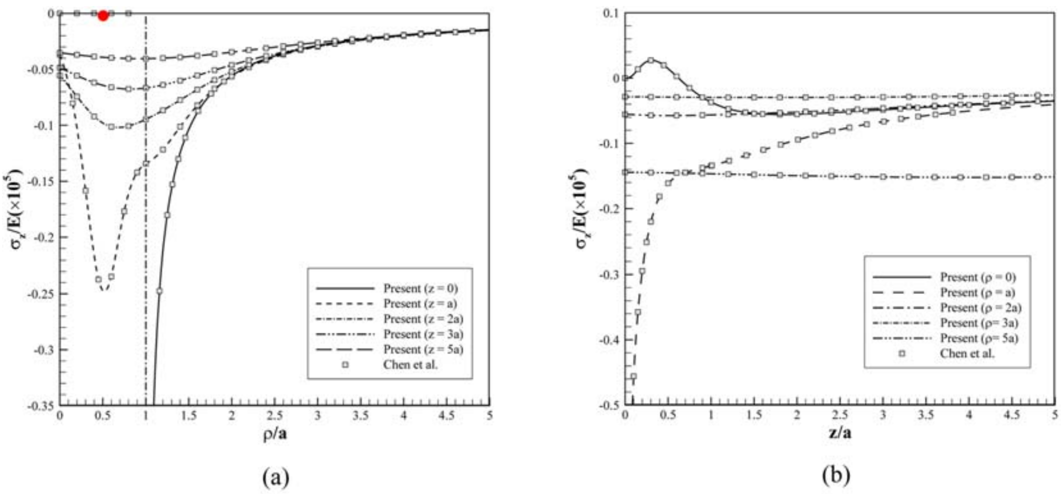

Fig. 3 The dimensionless stress $\sigma_Z/E(\times 10^5)$ as a function of (a) ρ/a and of (b) z/a. In (a), the mark (•) indicates the point where the concentrated force is applied. The corresponding σ_z/E is infinite, which can not be shown

Fig. 2 and Fig. 3 show the variation of the dimensionless temperature T/Θ_3^0 and the normal stress component σ_z/E with the spatial coordinates, respectively. It is seen that the present solutions agree well with those in Chen *et al.* (2004).

Table 2 lists the stress intensity factor K_I for various $(\phi-\phi_0)/\pi$ due to the thermal load. A good agreement is again observed in view of the negligible relative difference. By means of comparing various physical quantities in table and figure forms, the validity of the present solutions is achieved.

Table 2 Comparison of the stress intensity factor with those given by Chen *et al.* (2004)

$\frac{\phi-\phi_0}{\pi}$	$K_I \times 10^{-3}$		Relative error (%)
	Present	Chen *et al.* (2004)	
0.0	-5.71190263384547	-5.70405132152740	0.1374520
0.1	-4.77674128585335	-4.77017533116283	0.1374587
0.2	-3.23816495811846	-3.23371380476813	0.1374555
0.3	-2.15636353981846	-2.15339939024326	0.1374546
0.4	-1.51753616919305	-1.51545014709516	0.1374625
0.5	-1.14238059576696	-1.14081026739772	0.1374624
0.6	-0.915946229280748	-0.914687164452968	0.1374632
0.7	-0.777009023835998	-0.775940949346910	0.1374573
0.8	-0.693523031429236	-0.692569724526042	0.1374600
0.9	-0.648768296104223	-0.647876517956539	0.1374612
1.0	-0.634655848205055	-0.633783480169711	0.1374562

Note: Relative error is defined as $\frac{|\text{Present}-\text{Chen } et\ al.\ (2004)|}{|\text{Present}|}\times 100\%$

8.2 Effect of anisotropy

Once the correctness of the proposed solutions is confirmed, we can employ the solutions to analyze the effect of the physical parameters, among which E'/E and ν'/ν are of high significance. The following two subsections are devoted to influence of these two parameters, respectively. Under this situation, we exert three types of loads with the following magnitudes: $\Theta_1^0 = -1000\ \mathrm{N}$, $\Theta_2^0 = 101325\ \mathrm{Pa}$ and $\Theta_3^0 = 1\ ^{\circ}\mathrm{C}$. For readers' convenience, the loads $\Theta_j^0 (j=1,2,3)$ denote the force, pressure and temperature, respectively. It is noted that Θ_2^0 is a standard atmosphere in magnitude and these loads $\Theta_j^0 (j=1-3)$ are often encountered in practice.

In the following analyses, $K(\Theta_1^0,0,0), K(0,\Theta_2^0,0), K(0,0,\Theta_3^0)$ and $K(\Theta_1^0,\Theta_2^0,\Theta_3^0)$ represent the stress intensity factor due to the mechanical, pressure, thermal and the generalized mechanical loads, respectively. It is also noted that the displacement involved results from $\Theta_j^0 (j=1,2,3)$ applied at $(\rho_0, \phi_0) = (0.5a, 0)$ simultaneously, if not stated otherwise.

8.2.1 Influence of the ratio E′/E

To examine the influence of E'/E on the thermoporoelastic field, we treat E' as a variable while other material constants are identical to these in Table 1.

Fig. 4 plots the variation of the stress intensity factor K_I with E'/E. $K(\Theta_1^0,0,0)$ is not sensitive to the material constants. This observation has been made by Fabrikant (1989) for pure elasticity and by Chen and Ding (2004) for multi-field coupling materials. It is seen that $K(0,\Theta_2^0,0)$ and $K(0,0,\Theta_3^0)$ change significantly with E'/E; the sign of $K(0,\Theta_2^0,0)$ changes as E'/E increases. The resultant $K(\Theta_1^0,\Theta_2^0,\Theta_3^0)$ are therefore varies significantly with the Young's modulus E' along the z- direction.

Fig. 5 presents the distribution of the quantity $\lg[w(\rho,\phi,z)/w(0,\phi_0,0)]$ on the plane with $\phi = \phi_0$ for E'/E equal to 0.5, 1.0, 5 and 20. It is clearly shown that E'/E is an important parameter changing the pattern of the displacement. For completeness, the curve of $w(0,\phi_0,0)$ as a function of E'/E is given in Fig. 6, where significant changes are again observed, especially in the range $0 < E'/E \le 10$.

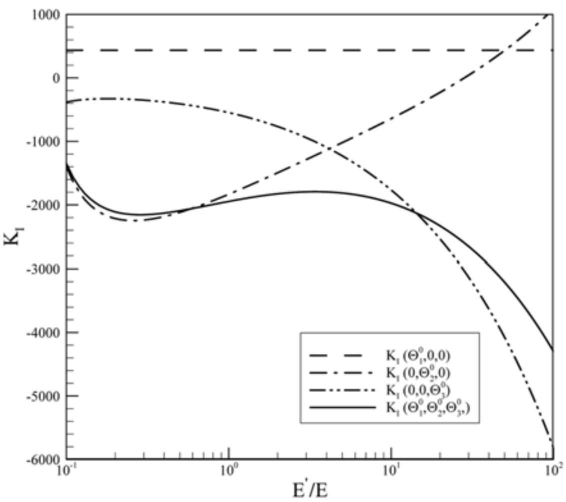

Fig. 4 The stress intensity factor K_I as a function of E'/E

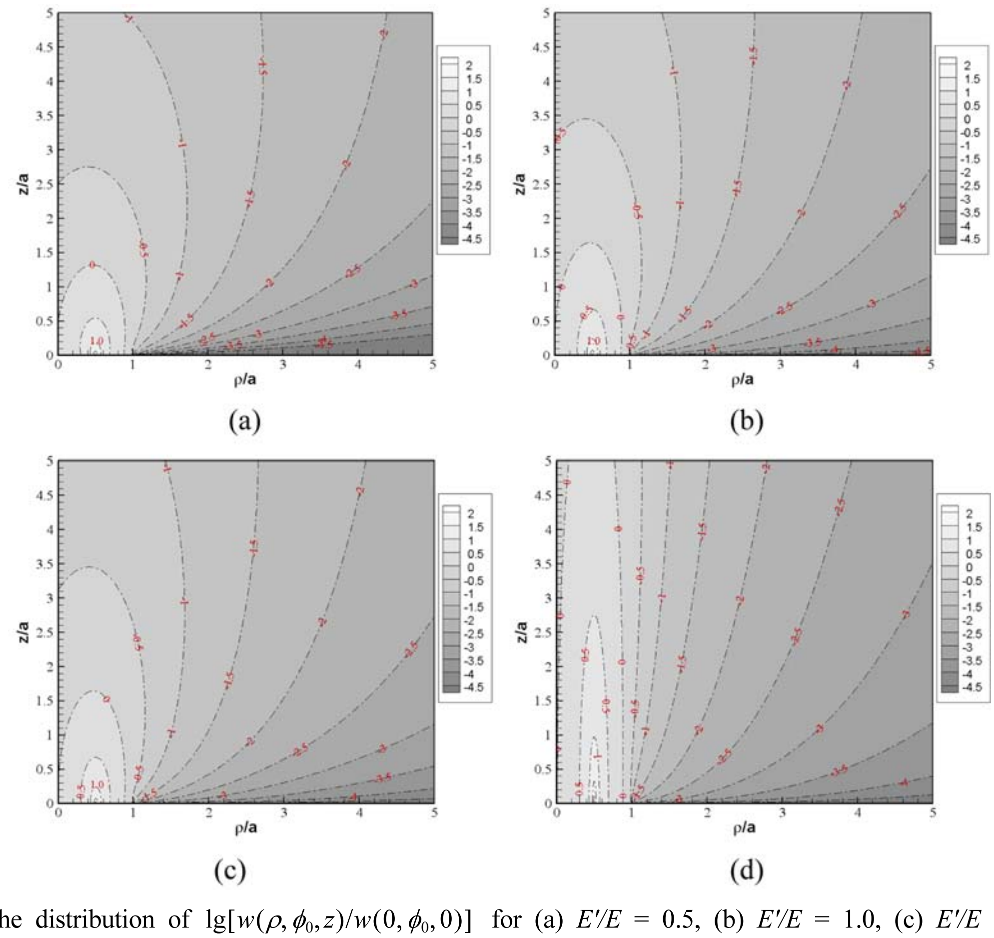

Fig. 5 The distribution of $\lg[w(\rho,\phi_0,z)/w(0,\phi_0,0)]$ for (a) $E'/E = 0.5$, (b) $E'/E = 1.0$, (c) $E'/E = 5$ and (d) $E'/E = 20$

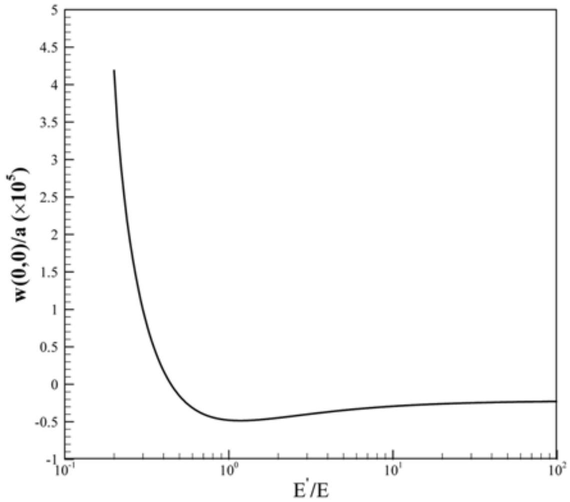

Fig. 6 The dimensionless displacement $w(0, \phi_0, 0)/a$ at the origin as a function of E'/E

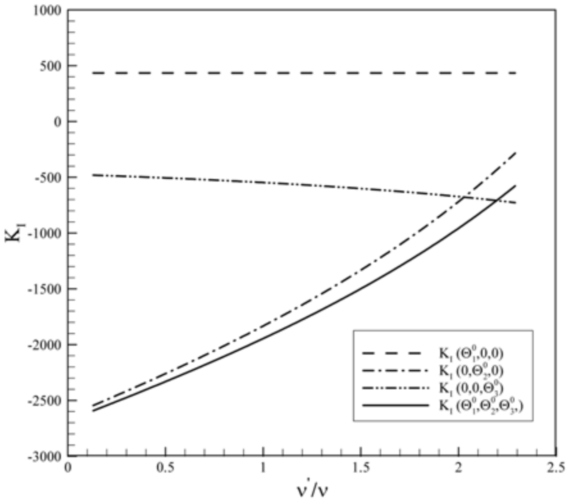

Fig. 7 The stress intensity factor K_I as a function of ν'/ν

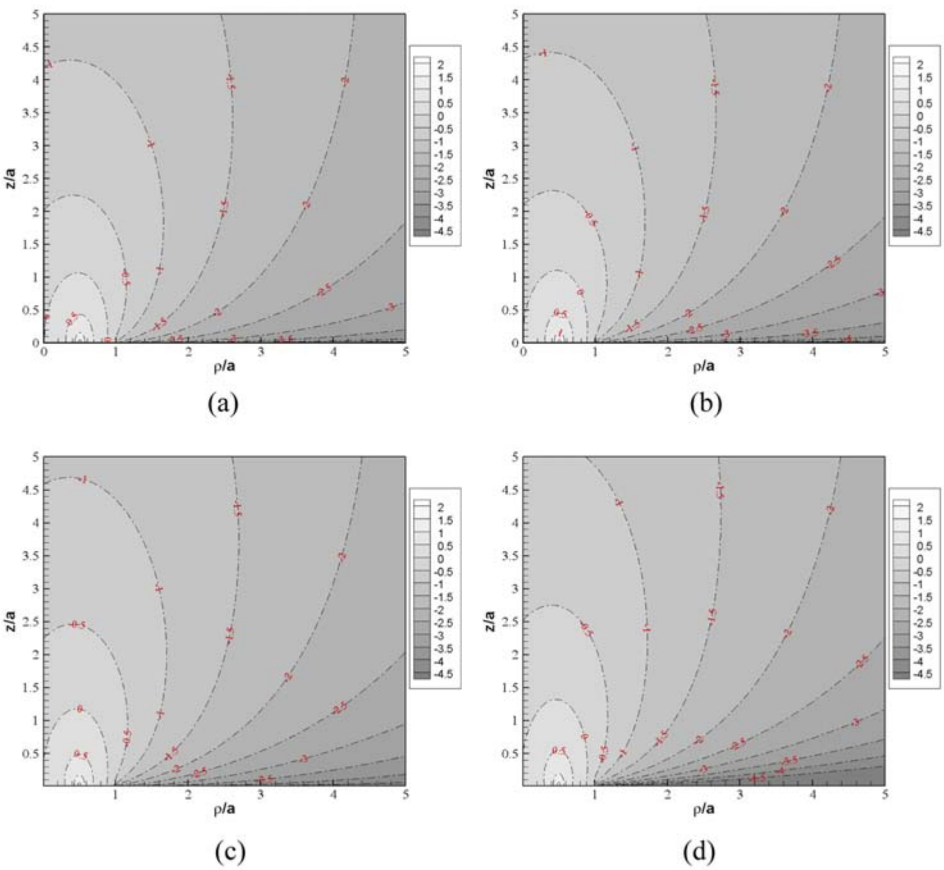

Fig. 8 The distribution of $\lg[w(\rho, \phi_0, z)/w(0, \phi_0, 0)]$ for (a) $\nu'/\nu = 0.1$, (b) $\nu'/\nu = 1.0$, (c) $\nu'/\nu = 1.5$ and (d) $\nu'/\nu = 2.0$ (d)

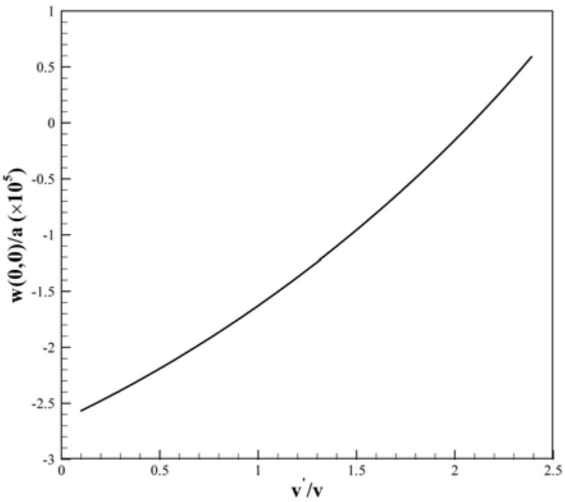

Fig. 9 The dimensionless displacement $w(0,\phi_0,0)/a$ at the origin as a function of ν'/ν

8.2.2 Influence of the ratio ν'/ν

In order to investigate the effect of the parameter ν'/ν, the material constants in Table 1 remain unchanged, except for ν' as a variable changing from 0 to 0.5. Parallel to the analyses in subsection 8.2.1, the dependency of K_I, $\lg[w(\rho,\phi,z)/w(0,\phi_0,0)]$ and $w(0,\phi_0,0)$ upon ν'/ν are given in Figs. 7, 8 and 9, respectively. All the physical quantities change significantly with ν'/ν, with an exception of $K(\Theta_1^0,0,0)$ which is a constant as expected.

From an overall point of view, the anisotropy of the materials has a significant influence on distributions of the thermoporoelastic field. Of course, the dependencies of the corresponding quantities upon ν'/ν are quite different from these upon E'/E (see Fig. 6 and Fig. 9, for example), since E'/E and ν'/ν are conceptually different parameters quantifying the anisotropy of the media.

9. Conclusions

In the present study, a penny-shaped crack problem is considered in the domain of thermoporoelasticity. By using the general thermoporoelastic solution recently proposed by Li *et al.* (2010) and the potential theory method, the exact and closed form fundamental solutions expressed in terms of elementary functions are derived. The validity of the present solutions is thoroughly discussed in analytic and numerical ways. By comparing with the results available in literature, an excellent agreement has been observed. Hence the solution in this paper can naturally serve as a benchmark to check various numerical codes and approximate theories. This point should be highlighted in view of the rareness of exact solutions in thermoporoelasticity.

Based on the present solutions, numerical simulations can be easily performed to analyze the influence of various physical parameters on the thermoporoelastic field, especially the singularity behavior at the crack tip. It is found that the anisotropy of the material has a significant influence on the thermoporoelastic field.

It should be pointed out that the potential theory method conjugated with the thermoporoelastic general solution (Li *et al.* 2010) can deal with mode II and III problems. Under that condition, the corresponding potential functions will take on a completely new form and extra mathematical difficulties will be encountered. This will be reported in another paper.

Acknowledgments

The work was supported by the National Natural Science Foundation of China (Nos. 10725210, 10832009 and 11102171), and the National Basic Research Program of China (No. 2009CB623204). The support by the Fundamental Research Funds for the Central Universities (No. SWJTU11CX069) is acknowledged as well. One author (Xiang-Yu LI) would like to express his sincere thanks to Professor H.J. Ding in Zhejiang University, who introduced him into the field of elasticity.

References

Abousleiman, Y. and Ekbote, S. (2000), "Porothermoelasticity in transversely isotropic porous materials", *IUTAM Symposium on Theoretical and Numerical Method in Continuum Mechanics of Porous Materials*, 145-152.

Abousleiman, Y., Cheng, A.H.D., Cui, L., Detournay, E. and Roegiers, J.C. (1996), "Mandel's problem revisited", *Géotechnique*, **46**, 187-195.

Adélaïde, F.F., Bui, H.D. and Ehrlacher, A. (2003), "Hydrostatic interaction of a wetting fluid and a circular crack in an elastic material", *Mech. Mater.*, **35**, 581-586.

Atkinson, C. and Craster, R.V. (1991), "Plane strain fracture in poroelastic media", *Proc. Roy. Soc. London*. **A434**, 605-633.

Biot, M.A. (1941), "General solutions of three-dimensional consolidation", *J. Appl. Phys.*, **12**, 155-164.

Biot, M.A. (1955), "Theory of elasticity and consolidation for a porous anisotropic solid", *J. Appl. Phys.*, **26**, 182-185.

Boone, T.J. and Detournay, E. (1990), "Response of a vertical hydraulic fracture intersecting a poroelastic formation bounded by a semi-infinite impermeable elastic layer", *Int. J. Rock. Mech. Min. Sci. Geomech. Abstr.*, **27**, 189-197.

Chen, J. (1994a), "Time domain fundamental solution to Biot's complete equations of poroelasticity: Part I two-dimensional solution", *Int. J. Solids Struct.*, **31**, 1447-1490.

Chen, J. (1994b), "Time domain fundamental solution to Biot's complete equations of poroelasticity: Part II three-dimensional solution", *Int. J. Solids Struct.*, **3**, 169-202.

Chen, W.Q. and Ding, H.J. (2004), "Potential theory method for 3D crack and contact problems of multi-field coupled media: A survey", *J. Zhejiang Univ. SCI.*, **5**(9), 1009-1021.

Chen, W.Q., Ding, H.J. and Ling, D.S. (2004), "Thermoelastic field of a transversely isotropic elastic medium containing a penny-shaped crack: exact fundamental solution", *Int. J. Solids Struct.*, **41**, 69-83.

Cheng, A.H.D. and Detournay, E. (1988), "A direct boundary element for plane strain poroelasticity", *Int. J. Numer. Anal. Meth. Geomech.*, **12**, 551-572.

Cheng, A.H.D. and Liggett, J.A. (1984a), "Boundary integral equation method for linear porous-elasticity with applications to soil consolidation", *Int. J. Numer. Meth. Eng.*, **20**, 255-278.

Cheng, A.H.D. and Liggett, J.A. (1984b), "Boundary integral equation method for linear porous-elasticity with applications to fracture propagation", *Int. J. Numer. Meth. Eng.*, **20**, 279-296.

Cleary, M.P. (1977), "Fundamental solutions for a fluid-saturated porous solid", *Int. J. Solids Struct.*, **13**, 785-806.

Coussy, O. (1995), *Poromechanics*, John Wiley & Sons, Ltd.

Ding, H.J., Chen, W.Q. and Zhang, L.C. (2006), *Elasticity of Transversely Isotropic Materials*, Springer, Dordrecht.

Fabrikant, V.I. (1989), "Applications of potential theory in mechanics: A selection of new results", Kluwer

Academic Publishers, The Netherlands.
Gatmiri, B. and Jabbari, E. (2005a), "Time-domain Green's functions for unsaturated soils. Part I: Two-dimensional solution", *Int. J. Solids Struct*., **42**, 5971-5990.
Gatmiri, B. and Jabbari, E. (2005b), "Time-domain Green's functions for unsaturated soils. Part II: Three-dimensional solution", *Int. J. Solids Struct*., **42**, 5991-6002.
Gatmiri, B. and Nguyen, K.V. (2005), "Time 2D fundamental solution for saturated porous media with incompressible fluid", *Commun. Numer. Meth. Eng*., **21**(3), 119-132.
Gibson, R.E. (1967), "Some results concerning displacements and stresses in a non-homogeneous elastic half-space", *Geotechnique*, **17**, 58-67.
Gibson, R.E. and McNamee, J. (1963), "A three-dimensional problem of consolidation of a semi-infinite clay stratum", *Quart. J. Mech. Appl. Math*., **16**, 115-127.
Gordeyev, Y.N. (1995), "A hydraulic fracture in a transversely isotropic poroelastic medium", *J. Appl. Math. Mech*., **59**, 645-656.
Gradsbteyn, I.S. and Ryzbik, L.M. (2004), *Table of Integrals, Series, and Products,* 6th edition, Elsevier, Pte. Ltd., Singapore.
Kanj, M. and Abousleiman, Y. (2005), "Porothermoelastic analyses of anisotropic hollow cylinders with applications", *Int. J. Numer. Anal. Meth. Geomech*., **29**, 103-126.
Li, X.Y., Chen, W.Q. and Wang, H.Y. (2010), "General steady state solutions for transversely isotropic thermoporoelastic media in three dimensions and its application", *Eur. J. Mech. A/Solids*, **29**, 317-326.
Liu, L. and Kardomateas, G.A. (2005), "Thermal stress intensity factors for a crack in an anisotropic half plane", *Int. J. Solids Struct*., **42**, 5208-5223.
Nowacki, W. (1966), "Green's functions for a thermoelastic medium (quasi-static problem)", Buletinul Institutului Politehnic din Iasi, Serie Noua12, 83-92.
Norris, A.N. (1985), "Radiation from a point source and scattering theory in a fluid-saturated porous solid", *J. Acoustic. Soc. Am*., **77**, 2012-2023.
Singh, B.M., Danyluk, H.T. and Selvachurai, A.P.S. (1987), "Thermal stresses in a transversely isotropic elastic solid weakened by an external circular crack", *Int. J. Solids Struct*., **23**, 403-412.

Appendix A

If we assume that the z-axis is perpendicular to the material symmetry plane in the Cartesian coordinates (x, y, z), the constitutive equations for a transversely isotropic thermoporoelastic medium read (Coussy 1995)

$$\sigma_x = c_{11}\frac{\partial u}{\partial x} + (c_{11} - 2c_{66})\frac{\partial v}{\partial y} + c_{13}\frac{\partial w}{\partial z} - \alpha_1 P - \beta_1 T, \quad \sigma_{yz} = c_{44}\left(\frac{\partial w}{\partial y} + \frac{\partial v}{\partial z}\right)$$

$$\sigma_y = (c_{11} - 2c_{66})\frac{\partial u}{\partial x} + c_{11}\frac{\partial v}{\partial y} + c_{13}\frac{\partial w}{\partial z} - \alpha_1 P - \beta_1 T, \quad \sigma_{zx} = c_{44}\left(\frac{\partial w}{\partial x} + \frac{\partial u}{\partial z}\right)$$

$$\sigma_z = c_{13}\left(\frac{\partial u}{\partial x} + \frac{\partial v}{\partial y}\right) + c_{33}\frac{\partial w}{\partial z} - \alpha_3 P - \beta_3 T, \quad \sigma_{xy} = c_{66}\left(\frac{\partial u}{\partial y} + \frac{\partial v}{\partial x}\right) \tag{A1}$$

where P and T are variations in the pore pressure and temperature, respectively; $P = 0$ and $T = 0$ correspond to the stress-free state; Conditional symbols $u(v, w)$ and σ_{ij} are used to denote components of displacement and stress, respectively; c_{ij}, $\alpha_1(\alpha_3, M)$ and $\beta_1(\beta_3, \beta_m)$ are elastic moduli, Biot's effective stress coefficients and thermal constants, respectively.

The material coefficients in Eqs. (A1) can be denoted by the engineering constants as follows (Kanj and Abousleiman 2005)

$$c_{11} = \frac{E(E' - E\nu'^2)}{(1+\nu)(E' - E'\nu - 2E\nu'^2)}, \quad c_{12} = \frac{E(E'\nu + E\nu'^2)}{(1+\nu)(E' - E'\nu - 2E\nu'^2)}$$

$$c_{13} = \frac{EE'\nu'}{E' - E'\nu - 2E\nu'^2}, \quad c_{33} = \frac{E'^2(1-\nu)}{E' - E'\nu - 2E\nu'^2}, \quad c_{44} = \frac{E'}{2(1+\nu')} \tag{A2}$$

where E is the drained Young's modulus in the plane of isotropy ($x-y$ plane), and E' the drained Young's modulus perpendicular to that plane, i.e., along the z-direction. Assuming that the solid skeleton is micro-homogeneous and micro-isotropic, we can express α_1 and α_3 in terms of c_{ij} and the bulk modulus of the solid grain K_s according to

$$\alpha_1 = 1 - \frac{c_{11} + c_{12} + c_{13}}{3K_s}, \quad \alpha_3 = 1 - \frac{2c_{13} + c_{33}}{3K_s} \tag{A3}$$

Furthermore β_1, β_3 and β_m are related to the linear expansion coefficients in the isotropic and transverse planes of the material (α_1 and α_3) and the volumetric expansion coefficient α_f of the pore fluid as

$$\beta_1 = (c_{11} + c_{12})\alpha_1^s + c_{13}\alpha_3^s, \; \beta_3 = 2c_{13}\alpha_1^s + c_{33}\alpha_3^s, \; \beta_m = 2\alpha_1\alpha_1^s + \alpha_3\alpha_3^s + (\alpha_f - 2\alpha_1^s - \alpha_3^s)\phi' \tag{A4}$$

where ϕ' is the porosity.

Appendix B

Here, we present the constants involved in the general solution.

In Eq. (4), the constants are defined as

$$\mu_{i1} = \eta_{i2}s_i / \eta_{i1}, \; \mu_{ij} = \eta_{i(j+1)}(\delta_{j2} + \delta_{j3})(\delta_{i3} + \delta_{i4}) / \eta_{i1} \quad j = 2,3, \; i = 1-4 \tag{B1}$$

where δ_{ij} is the Kronecker delta, and

$$\eta_{ij} = a_j s_i^4 - b_j s_i^2 + c_j (j = 1,2), \quad \eta_{3n} = (a_0 s_n^4 - b_0 s_n^2 + c_0)(\lambda_{33} s_n^2 - \lambda_{11})$$

$$\eta_{4n} = (a_0 s_n^4 - b_0 s_n^2 + c_0)(\kappa_{33} s_n^2 - \kappa_{11}), \; (n = 3-4) \tag{B2}$$

with

$$\begin{gathered}
a_0 = c_{33}c_{44},\ b_0 = c_{11}c_{33} + c_{44}^2 - (c_{13}+c_{44})^2,\ \ c_0 = c_{11}c_{44} \\
a_1 = (c_{13}+c_{44})(\kappa_{33}\beta_3 + \lambda_{33}\alpha_3) - c_{33}(\kappa_{33}\beta_1 + \lambda_{33}\alpha_1) \\
b_1 = (c_{13}+c_{44})(\kappa_{11}\beta_3 + \lambda_{11}\alpha_3) - c_{44}(\kappa_{33}\beta_1 + \lambda_{33}\alpha_1) - c_{33}(\kappa_{11}\beta_1 + \lambda_{11}\alpha_1) \\
c_1 = -c_{44}(\kappa_{11}\beta_1 + \lambda_{11}\alpha_1),\ a_2 = c_{44}(\kappa_{33}\beta_3 + \lambda_{33}\alpha_3) \\
b_2 = c_{11}(\kappa_{33}\beta_3 + \lambda_{33}\alpha_3) + c_{44}(\kappa_{11}\beta_3 + \lambda_{11}\alpha_3) - (c_{13}+c_{44})(\kappa_{33}\beta_1 + \lambda_{33}\alpha_1) \\
c_2 = c_{11}(\kappa_{11}\beta_3 + \lambda_{11}\alpha_3) - (c_{13}+c_{44})(\kappa_{11}\beta_1 + \lambda_{11}\alpha_1) \\
a_3 = a_0\lambda_{33},\ \ b_3 = a_0\lambda_{11} + b_0\lambda_{33},\ \ c_3 = b_0\lambda_{11} + c_0\lambda_{33},\ d_3 = c_0\lambda_{11} \\
a_4 = a_0\kappa_{33},\ \ b_4 = a_0\kappa_{11} + b_0\kappa_{33},\ \ c_4 = b_0\kappa_{11} + c_0\kappa_{33},\ d_4 = c_0\kappa_{11}
\end{gathered} \tag{B3}$$

The constants in Eq. (7) read

$$\begin{gathered}
\gamma_{j1} = c_{13} + c_{33}\mu_{j1}s_j - \alpha_3\mu_{j2} - \beta_3\mu_{j3} \\
\gamma_{j2} = 2\left[c_{11} - c_{16} + c_{13}\mu_{j1}s_j - \alpha_1\mu_{j2} - \beta_1\mu_{j3}\right] \\
\gamma_{j3} = c_{44}(\mu_{j1} - s_j),\ \ j = 1-4
\end{gathered} \tag{B4}$$

It is noted that the identity $\gamma_{j3} = \gamma_{j1}s_j,\ (j = 1-4)$ holds.

Appendix C

The derivatives of the Green's function Π_1 read (Fabrikant 1989)

$$\Lambda\Pi_1 = -2\pi f_1(z) = -\frac{2\pi}{\bar{t}}\left[-\frac{z}{R_0}\tan^{-1}\left(\frac{h}{R_0}\right) + \frac{\sqrt{a^2-\rho_0^2}}{\bar{s}}\tan^{-1}\left(\frac{\bar{s}}{\sqrt{l_2^2-a^2}}\right)\right]$$

$$\frac{\partial\Pi_1}{\partial z} = -2\pi f_2(z) = -\frac{2\pi}{R_0}\tan^{-1}\left(\frac{h}{R_0}\right)$$

$$\frac{\partial^2\Pi_1}{\partial z^2} = -2\pi f_3(z) = -2\pi\left[-\frac{z}{R_0^3}\tan^{-1}\left(\frac{h}{R_0}\right) + \frac{h}{z(R_0^2+h^2)}\left(\frac{\rho^2-l_1^2}{l_2^2-l_1^2} - \frac{z^2}{R_0^2}\right)\right]$$

$$\begin{aligned}
\Lambda^2\Pi_1 &= -2\pi f_4(z) \\
&= -2\pi\left\{\frac{\sqrt{a^2-\rho_0^2}}{\bar{t}\bar{s}}\left(\frac{\rho_0 e^{\mathrm{i}\phi_0}}{\bar{s}^2} - \frac{2}{\bar{t}}\right)\tan^{-1}\left(\frac{\bar{s}}{\sqrt{l_2^2-a^2}}\right)\right. \\
&\quad + \frac{z(3R_0^2-z^2)}{\bar{t}^2R_0^3}\tan^{-1}\left(\frac{h}{R_0}\right) - \frac{\sqrt{a^2-\rho_0^2}\sqrt{l_2^2-a^2}\,\rho_0 e^{\mathrm{i}\phi_0}}{\bar{t}\bar{s}^2[l_2^2-\rho\rho_0 e^{-\mathrm{i}(\phi-\phi_0)}]} \\
&\quad \left. + \frac{zh}{R_0^2+h^2}\left[\frac{t}{\bar{t}R_0^2} - \frac{\rho^2 e^{\mathrm{i}2\phi}}{(l_2^2-l_1^2)(l_2^2-\rho^2)}\right]\right\}
\end{aligned}$$

$$\Lambda\frac{\partial\Pi_1}{\partial z} = -2\pi f_5(z) = 2\pi\left[\frac{t}{R_0^3}\tan^{-1}\left(\frac{h}{R_0}\right) + \frac{h}{R_0^2+h^2}\left(\frac{\rho e^{\mathrm{i}\phi}}{l_2^2-l_1^2} + \frac{t}{R_0^2}\right)\right] \tag{C1}$$

where

$$t=\rho e^{\mathrm{i}\phi}-\rho_0 e^{\mathrm{i}\phi_0},\ \bar{s}=\sqrt{a^2-\rho\rho_0 e^{-\mathrm{i}(\phi-\phi_0)}},\ h=\sqrt{a^2-l_1^2}\sqrt{a^2-\rho_0^2}\,/\,a$$
$$R_0=\sqrt{\rho^2+\rho_0^2-2\rho\rho_0\cos(\phi-\phi_0)+z^2}$$
$$l_1=l_1(\rho,z)=\tfrac{1}{2}[\sqrt{(\rho+a)^2+z^2}-\sqrt{(\rho-a)^2+z^2}]$$
$$l_2=l_2(\rho,z)=\tfrac{1}{2}[\sqrt{(\rho+a)^2+z^2}+\sqrt{(\rho-a)^2+z^2}] \tag{C2}$$

The derivatives of Π_2 are listed as follows (Chen *et al*. 2004)

$$\Lambda\Pi_2=g_1(z)=\frac{1}{\bar{t}}\left\{\frac{z}{R_0}\tan^{-1}\left(\frac{h}{R_0}\right)-\frac{z}{h}\right.$$
$$+\frac{1}{\sqrt{a^2-\rho_0^2}}\left[\sqrt{a^2-\rho^2/\varsigma}\tan^{-1}\left(\frac{a\sqrt{\rho^2-l_1^2}}{l_1\sqrt{a^2-\rho^2/\varsigma}}\right)\right.$$
$$\left.\left.+\frac{\pi}{2}\sqrt{a^2-\rho^2/\bar{\varsigma}}-\frac{z}{\sqrt{\bar{\varsigma}-1}}\tan^{-1}\left(\frac{\sqrt{a^2-l_1^2}}{a\sqrt{\bar{\varsigma}-1}}\right)\right]\right\}$$

$$\frac{\partial\Pi_2}{\partial z}=g_2(z)=-\frac{1}{R_0}\tan^{-1}\left(\frac{h}{R_0}\right)+\frac{1}{\sqrt{a^2-\rho_0^2}}\left[\ln\left(\frac{a+\sqrt{a^2-l_1^2}}{l_1}\right)\right.$$
$$\left.+\frac{1}{\sqrt{\varsigma-1}}\tan^{-1}\left(\frac{\sqrt{a^2-l_1^2}}{a\sqrt{\varsigma-1}}\right)+\frac{1}{\sqrt{\bar{\varsigma}-1}}\tan^{-1}\left(\frac{\sqrt{a^2-l_1^2}}{a\sqrt{\bar{\varsigma}-1}}\right)\right]$$

$$\frac{\partial^2\Pi_2}{\partial z^2}=g_3(z)=\frac{z}{R_0^3}\left[\frac{R_0}{h}+\tan^{-1}\left(\frac{h}{R_0}\right)\right]$$

$$\Lambda^2\Pi_2=g_4(z)$$
$$=-\frac{z(3R_0^2-z^2)}{\bar{t}^2R_0^3}\tan^{-1}\left(\frac{h}{R_0}\right)$$
$$+\frac{z}{\bar{t}}\left[\frac{2}{\bar{t}h}-\frac{ht}{R_0^2(R_0^2+h^2)}\right]-\frac{z\,\mathrm{e}^{\mathrm{i}\phi}(\rho^2-\rho_0^2\varsigma)}{\bar{t}h\rho(R_0^2+h^2)}$$
$$-\frac{1}{\bar{t}^2}\left(\frac{\sqrt{a^2-\rho_0^2}}{\sqrt{a^2-\rho^2/\varsigma}}+\frac{\sqrt{a^2-\rho^2/\varsigma}}{\sqrt{a^2-\rho_0^2}}\right)\tan^{-1}\left(\frac{a\sqrt{\rho^2-l_1^2}}{l_1\sqrt{a^2-\rho^2/\varsigma}}\right)$$
$$+\frac{3z}{\bar{t}^2\sqrt{a^2-\rho_0^2}\sqrt{\bar{\varsigma}-1}}\tan^{-1}\left(\frac{\sqrt{a^2-l_1^2}}{a\sqrt{\bar{\varsigma}-1}}\right)$$
$$+\frac{z}{\bar{t}^2h}\left[\frac{l_1^2(1-1/\bar{\varsigma})}{a^2\varsigma-l_1^2}+\frac{a^2-l_1^2}{a^2\bar{\varsigma}-l_1^2}\right]-\frac{\pi}{\bar{t}^2\sqrt{a^2-\rho_0^2}}\sqrt{a^2-\rho^2/\bar{\varsigma}},$$

$$\Lambda\frac{\partial \Pi_2}{\partial z} = g_5(z) = \frac{t}{R_0^3}\tan^{-1}\left(\frac{h}{R_0}\right) - \frac{z^2}{h\bar{t}R_0^2} - \frac{1}{\sqrt{a^2-\rho_0^2\bar{t}}\sqrt{\bar{\varsigma}-1}}\tan^{-1}\left(\frac{\sqrt{a^2-l_1^2}}{a\sqrt{\bar{\varsigma}-1}}\right) \tag{C3}$$

with $\varsigma = (\rho/\rho_0)e^{i(\phi-\phi_0)}$.